WARSAW UNIVERSITY OF TECHNOLOGY Index 351733
FACULTY OF CIVIL ENGINEERING
COMMITTEE FOR CIVIL AND WATER ENGINEERING
POLISH ACADEMY OF SCIENCES ISSN 1230-2945

DOI: 10.24425/ace.2023.147676

ARCHIVES OF CIVIL ENGINEERING

Vol. LXIX ISSUE 4 2023

pp. 549 –571

Research paper

Deformation failure analysis and identification method of zoning type of actual tunnel surrounding rock

Wei Jing[1], Yunlong Gao[2], Rencai Jin[3], Laiwang Jing[4]

Abstract: The research on deformation zoning mechanism of tunnel surrounding rock is of great significance for ensuring safe production and disaster prevention in coal mines. However, the traditional deformation zoning theory of tunnel surrounding rock uses the ideal strain softening model as the criterion for judging the zoning type of all tunnel surrounding rock, ignoring the difference between the deformation zoning type of a specific actual tunnel and the basic zoning type of surrounding rock. In order to study the method for determining the actual deformation zoning type of tunnel surrounding rock, the formation mechanism of the actual deformation zoning of tunnel surrounding rock has been revealed. Combined with engineering examples, a method for determining the actual deformation zoning type and boundary stress of specific tunnel surrounding rock has been proposed. The results show that the boundary stress and position of the actual deformation zone are determined by the peak strength fitting line, residual strength fitting line, support strength line, and the position of the circumferential and radial stress relationship lines of each deformation zone. The actual boundary stress of each zone of tunnel surrounding rock is ultimately only related to the basic mechanical properties of the tunnel surrounding rock and the in-situ stress field. The research results can provide reference for disaster management of underground engineering, stability evaluation of surrounding rock, and support scheme design.

Keywords: deformation mechanism, in-situ stress field, mechanical properties of surrounding rock, tunnel, zoning type, zone boundary stress

[1]Prof., PhD., Eng., Anhui University of Science and Technology, State key Laboratory of Mining response and disaster Prevention and Control in Deep Coal Mines, 168 Taifeng Street, Huainan City, Anhui Province, China, e-mail: wjing@aust.edu.cn, ORCID: 0000-0002-0256-7655

[2]B. Eng., Anhui University of Science and Technology, School of Civil Engineering and Architecture, 168 Taifeng Street, Huainan City, Anhui Province, China, e-mail: yunlonggao2000@163.com, ORCID: 0009-0008-4461-6858

[3]Eng., China MCC17 Group Co., LTD., Civil Engineering Post-doctoral Research Worktation, No. 88 Yushan East Road, Huashan District, Ma'anshan City, Anhui Province, China, e-mail: zgsqy17@sina.com, ORCID: 0000-0002-8028-3658

[4]Prof., PhD., Eng., Anhui University of Science and Technology, State key Laboratory of Mining response and disaster Prevention and Control in Deep Coal Mines, 168 Taifeng Street, Huainan City, Anhui Province, China, e-mail: lwjing229@126.com, ORCID: 0000-0003-3131-8786

1. Introduction

The quantitative design of tunnel surrounding rock support parameters has long been a hot research topic in deep rock mechanics [1–5]. Because of the lack of theories and methods to determine the actual deformation zoning type and zoning boundary position of surrounding rock, this research direction has always been a difficulty for scholars. With the increase of coal mining depth, the previous support design schemes often cannot ensure the long-term stability of surrounding rock. Various disasters and repeated maintenance problems such as tunnel roof fall, floor heave and roof collapse have always affected the personal safety of mining staff and the production efficiency of enterprises, and will also cause damage to the surface and underground ecological environment, It does not conform to the current green mining concept.

R. Fenner and J. Talobre put forward the "two-zone theory" theory of surrounding rock deformation based on the ideal elastic-plastic model [6]. On this basis, many scholars have further improved the "two-zone theory" [7–12]. However, with the appearance of fracture zone of tunnel surrounding rock and the deformation and failure properties of rock in the residual stage of complete stress-strain curve, the "two-zone theory" cannot be applied to the deformation mechanism analysis of surrounding rock of deep high stress tunnel, so the "three-zone theory" began to appear. The foundation of "three-zone theory" is the deformation of three properties reflected by the complete stress-strain curve of rock. At present, many research results are based on the "three-zone theory". Based on the strain softening characteristics of rock mass, Ma et al. [13], Fahimifar et al. [14], Yao et al. [15], Walton et al. [16] and Paul et al. [17] presented the stress distribution law of elastic zone, plastic zone and fracture zone of soft rock tunnel and the analytical solution of boundary position of each zone. Chen et al. [18], Zhang et al. [19] and Sun et al. [20] consider the influence of intermediate principal stress and rock mass expansion characteristics, and derive the analytical solutions of stress, deformation and plastic zone radius of three deformation zones of surrounding rock of deep circular tunnel. Zou et al. [21] divided the stress distribution around the cavity expansion into three zones (elastic zone, softening zone and plastic flow zone), and considered the factors of large strain, drainage condition and intermediate principal stress, so as to obtain the softening zone radius of strain softening soil, the closed solution of stress and strain in different zones, and the excess pore water pressure and limit cavity expansion pressure in plastic flow zone. Yao et al. [22] and Pan et al. [23] put forward the theoretical solution of stress and displacement in each zone of soft rock tunnel based on the characteristics of plastic softening and dilatancy of rock mass. Alejano et al. [24] divided the surrounding rock into three zones, proposed a simplified approximate formula for the plastic radius of tunnel excavation in strain softening rock mass, and obtained a more practical calculation method of longitudinal deformation profile of strain softening rock mass.

In addition to these representative results, there are many related achievements [25–28]. Although these achievements have promoted the great development of this research field, there are still some problems in the two zoning theories that need to be further studied and improved, which can be summarized in four aspects: (1) There is no in-depth study

on the key role of the two major factors of surrounding rock properties and in-situ stress in the study of surrounding rock deformation zoning types. In the analytical solution of some results, although the parameters of surrounding rock properties and in-situ stress are introduced into the calculation formula of plastic zone radius, and no matter how these two parameters are selected, the plastic zone radius has an analytical solution [29–31]. But in fact, the number of analytical expressions of radius directly depends on the actual number of surrounding rock zones. (2) The essential difference between the basic deformation zoning type and the actual deformation zoning type is not revealed. The theories of "two-zone" and "three-zone" mentioned above are essentially the basic deformation zoning types of surrounding rock, but most of the previous studies directly regarded the basic deformation zoning type as the actual deformation zoning type, which leads to the inaccuracy of the relevant calculation results. This is an important reason why the support problem of deep tunnel has not been well solved. In this paper, the basic deformation zoning type is defined as the deformation zoning type when the number of zones reaches the limit value (the zoning type when the broken zone appears in the surrounding rock), and the actual deformation zoning type is defined as the actual deformation zoning in the surrounding rock corresponding to the specific properties of surrounding rock and the in-situ stress field. Therefore, the number of actual deformation zoning type zones can only be less than or equal to the basic deformation zoning type zones. (3) In the past analytical research, the method of determining the actual deformation zoning type has not been given, but the determination of the actual deformation zoning type and boundary position is the basis for the quantitative design of surrounding rock support. (4) The difference between the complete stress-strain curve of rock and the stress-strain curve of tunnel surrounding rock along the radial direction is ignored. The strain softening model derived from the complete stress-strain curve is directly used as the basis for the deformation zoning of surrounding rock, and the results obtained from relevant research based on this theory are not accurate enough.

In view of the above four problems, this paper revealed the formation mechanism of the actual deformation zoning type of surrounding rock by analyzing the difference between the test loading path of surrounding rock specimen and the actual loading path of surrounding rock in the process of tunnel formation. Taking Huainan mining area in Anhui Province in Southeast China as an example, the actual deformation zoning type of tunnel surrounding rock and the determination method of each zoning boundary stress are deeply studied by means of the combination of test and theory. At the same time, the influence law of surrounding rock properties and in-situ stress field on the actual deformation zoning type and quantity of tunnel surrounding rock were analyzed.

2. Basic assumptions

In order to give a method to identify the actual deformation zoning type of surrounding rock, which is easy to understand and calculate, the tunnel surrounding rock and in-situ stress environment are idealized here in order to simplify the process of solving the problem,

which is also the basic method followed by theoretical analysis of coal mine tunnels for a long time [32–35]. This "idealization" is usually realized by setting a series of basic assumptions, the basic assumptions set in this paper are as follows.

1. It is assumed that the tunnel is a plane strain problem. Generally, the size of the tunnel along the axial direction is much larger than the cross-section size of the tunnel, and the surrounding rock properties and stress environment along the axial direction of the tunnel are basically unchanged, so it can be treated as a plane strain problem.

2. The pre-peak stage of the complete stress-strain curve is considered to be the ideal linear elastic stage, and the elastic modulus of rock is equal under different confining pressures. On this basis, it is assumed that the slope of the line between the peak point of the complete stress-strain curve and the coordinate origin is the elastic modulus of the ideal linear elastic stage, as shown in Fig. 1. Therefore, the relationship between stress and strain satisfies the following relationship:

$$\sigma_\theta - \sigma_\rho = E\varepsilon_\theta \tag{2.1}$$

Among them, σ_ρ and σ_θ are the radial stress and circumferential stress of tunnel surrounding rock, respectively. ε_θ is the circumferential strain of tunnel surrounding rock.

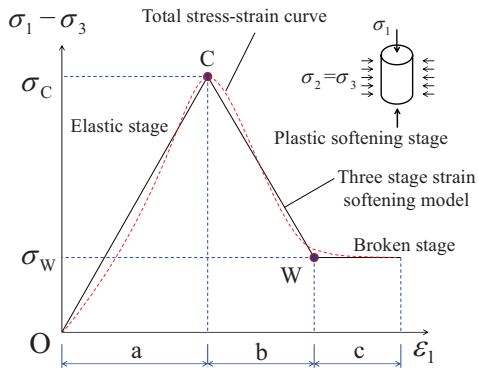

Fig. 1. Three-stage strain softening model of rock total stress-strain curve where a, b and c represent the elastic zone, plastic softening zone, and broken zone, respectively

As can be seen from the above formula, it is obvious that $\sigma_1 - \sigma_3$ is directly proportional to ε_1. Because the elastic modulus of rocks under different stress states has been approximately regarded as the same in rock mechanics, the pre-peak stage of the three-stage strain softening model under different confining pressures in the coordinate plane can be approximately regarded as coincident (collinear), as shown in Figs. 4–6.

3. The Mohr–Coulomb criterion is used for calculation without considering the influence of intermediate principal stress

For the surrounding rock of tunnel, the influence of intermediate principal stress is not considered, which means that only the effect of circumferential stress and radial stress in tunnel surrounding rock is considered, and the triaxial test is carried out with radial stress as confining pressure to study the stress distribution law of surrounding rock.

3. Zoning mechanism of actual deformation of surrounding rock

3.1. Division of basic deformation zoning type of surrounding rock

According to the research results of many scholars on the basic deformation zoning of surrounding rock, there are two common types of basic deformation zoning: "two-zone" type and "three-zone" type. Among them, "three-zone" type is the most widely used basic deformation zone type at present. Therefore, taking the "three-zone" basic deformation zoning type as an example, this paper divides the surrounding rock into elastic zone, plastic softening zone and broken zone to analyze the zoning mechanism of the actual deformation corresponding to this basic deformation zone type, On this basis, the determination method of the corresponding actual deformation zoning type is proposed. The mechanical model of tunnel surrounding rock corresponding to the basic deformation zoning type of "three-zone" is shown in Fig. 2.

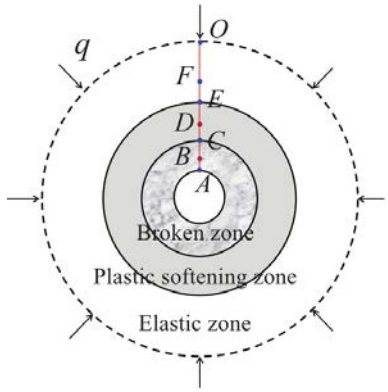

Fig. 2. Mechanical model of surrounding rock of axisymmetric tunnel

It should be emphasized that the actual deformation zoning type of surrounding rock is relative to the basic deformation zoning type. The basic deformation zoning type is "three zones", and the corresponding actual deformation zoning type may be one of three zones, two zones and one zone. The actual situation is which type needs to comprehensively analyze the test loading path of rock specimen and the actual loading path of surrounding rock path.

3.2. The loading path of tunnel surrounding rock

The complete stress-strain curve of rock specimen reflects the complete loading path of rock specimen from loading to complete crushing on the testing machine [36, 37]. A large number of test results [38] show that the total stress-strain curves under different confining pressures have an obvious feature, which is the ultimate compressive strength

(peak stress) and residual strength will gradually increase, and the strain value at the initial point of residual stage will gradually increase, so the test loading path corresponding to the complete stress-strain curves under different confining pressures is different inequality. It can be seen that the tunnel surrounding rock at different radial positions will correspond to different test loading paths due to different radial stress. Because there are countless points in the radial direction of the surrounding rock, there are countless test loading paths with different confining pressure corresponding to these points. In view of the axisymmetric tunnel surrounding rock illustrated in Fig. 3, a radial line segment AO is arbitrarily selected and 7 points A, B, C, D, E, F and O are selected on it. Obviously, the complete stress-strain curves corresponding to the rocks at these 7 positions will be different due to different confining pressures. The relevant schematic diagram is shown in Fig. 3.

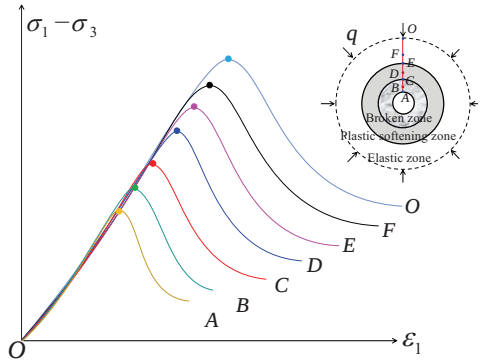

Fig. 3. Variation of complete stress-strain curve with confining pressure

The actual loading path refers to the distance that the rock in a certain part of the surrounding rock actually travels along its corresponding full stress-strain curve (test loading path) from the beginning of tunnel formation to the end of surrounding rock deformation [39, 40]. It can be seen from Fig. 3 that only point A in the mechanical model may go through a complete loading path, which means that the actual loading path of point A may be completed with its corresponding test loading path, and the other points can not go through the complete test loading path. Therefore, at the end of secondary stress adjustment (when the loading stops), the rock at different positions will stay at different positions in the corresponding test loading path (complete stress-strain curve), so the test loading path is essentially different from the actual loading path. To sum up, the ultimate deformation degree of the corresponding rock is different with the actual loading path.

3.3. Deformation characteristics of zoning types of surrounding rock

The determination of actual deformation zoning type mainly depends on the position of the rock at inner edge of the tunnel on the test loading path at the end of loading (the end position of the actual loading path). Because the three-stage strain softening model is the result of the simplification of the complete stress-strain curve and reflects the three

deformation stages with different properties in the whole loading process of rock specimen, so it can be regarded as an ideal test loading path. Accordingly, the three-stage strain softening model will be used as the complete loading trajectory of tunnel surrounding rock to study the formation mechanism of the actual deformation zoning type of surrounding rock.

3.3.1. Establishment of three-stage strain softening model group

The three-stage strain softening model group refers to a combination of these models under different confining pressures, all represented in the same coordinate plane. According to the drawing method of three-stage strain softening model, the three-stage strain softening model corresponding to seven full stress-strain curves A, B,C, D, E, F and O shown in Fig. 3 can be represented by 1, 2, 3, 4, 5, 6 and 7 in Fig. 4. Due to the fact that the 7 points A, B,C, D, E, F and O selected in Fig. 3 are distributed in all areas of the surrounding rock of the tunnel, it can fully reflect the deformation characteristics of each zone of the surrounding rock. It should be emphasized that these seven three-stage strain softening models are idealized models, and because of the mechanical properties of rock, these three-stage strain softening models should have the following three characteristics.

1. The pre-peak stages coincide with each other. This feature is derived from the above basic assumptions. According to the above basic assumptions, the pre-peak stage of the seven strain softening models in Fig. 4 is coincident.

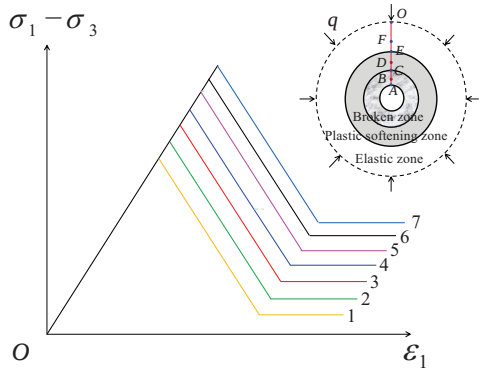

Fig. 4. Three-stage strain softening model group

2. The post-peak stage is approximately parallel. A large number of rock triaxial compression tests show that the greater the confining pressure, the greater the peak stress and the greater the residual strength. When the confining pressure is close to the peak stress, the post-peak stage presents a nearly horizontal feature, and the residual strength is approximately equal to the peak stress. Therefore, in the coordinate plane, the greater the confining pressure, the higher the position of the post-peak stage, and the smaller the angle between the post-peak stage and the horizontal axis. However, when the difference of confining pressure is small, the change of the angle between

the post-peak stage and the horizontal axis will be very small, which leads to the approximate parallel relationship among the post-peak stages corresponding to the three-stage strain softening model under different confining pressure. The difference of radial stress in the area within the boundary of the elastic zone of tunnel surrounding rock is generally less than 20 MPa, and the difference is very small, so it can be approximately considered that the post-peak stage of the three-stage strain softening model corresponding to each point in this area is approximately parallel.

3. The residual stages are all horizontal and straight lines. In the residual strength stage, the rock strength no longer decreases.

3.3.2. Deformation mechanism of surrounding rock in three zones

From the above analysis, it can be seen that the seven full stress-strain curves selected in the model represent the deformation paths of various zones of the surrounding rock of the entire tunnel. Therefore, the three-stage strain softening models 1, 2, 3, 4, 5, 6 and 7 corresponding to points A, B, C, D, E, F and O in Fig. 5 should show the law in Fig. 4.

In Fig. 5, when the loading end point position of point A corresponds to A' on the loading path 1 in Fig. 4, because point A' is already in the residual stage of the loading path 1, it can be determined that the inner edge of the tunnel has been in the range of the broken zone.

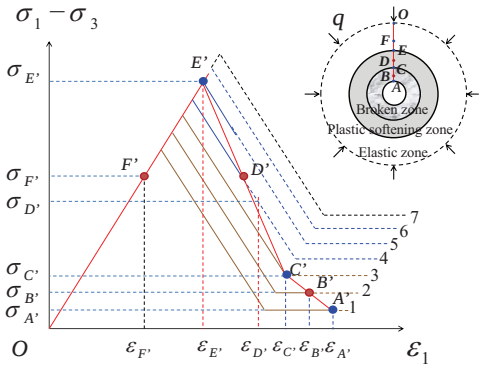

Fig. 5. Deformation mechanism of actual surrounding rock in three zones

In Fig. 5, each point in the radial direction of the mechanical model of tunnel surrounding rock has a coordinate point corresponding to it one by one in the coordinate plane, such as point A corresponds to $A'(\varepsilon_{A'}, \sigma_{A'})$, point$C$ corresponds to $C'(\varepsilon_{C'}, \sigma_{C'})$, point D corresponds to $D'(\varepsilon_{D'}, \sigma_{D'})$, point E corresponds to $E'(\varepsilon_{E'}, \sigma_{E'})$, point F corresponds to $F'(\varepsilon_{F'}, \sigma_{F'})$, the coordinate of point O is (0, 0).

In the model shown in Fig. 5, point C is located at the interface between the broken zone and the plastic softening zone, and point E is located at the interface between the plastic softening zone and the elastic zone. Therefore, the point C corresponding to point C' in the model must be located at the intersection of residual stage and the plastic softening stage in the corresponding model 3, that is, at the beginning of the residual stage

in model 3. Similarly, point E' must be at the beginning of the plastic softening stage in model 5. Connecting two points A' and C' and two points C' and E' in the coordinate plane, the idealized stress-strain relationship $O'E'C'A'$ of the surrounding rock along the radial direction of the axisymmetric circular tunnel can be obtained, that is, the strain softening model of surrounding rock along the radial direction of the tunnel. It should be emphasized here that both the straight lines $A'C'$ and $C'E'$ are idealized straight lines, and the actual connection is not necessarily a straight line, but may be some kind of curve, but because the parallel distance between the plastic softening stage and residual stage of model 3 and model 5 is very small, it is feasible to take the connection between two points A' and C' and between two points C' and E' as straight lines directly. The strain softening model of surrounding rock established in this way can clearly reflect the zones with three kinds of deformation properties in the surrounding rock from inside to outside. Because any point on the line $A'C'$ is in the residual stage in the corresponding loading path, the points corresponding to the line $A'C'$ in the surrounding rock must have been broken, so the area formed by these points must be the broken zone. Similarly, the points corresponding to $C'E'$ in the surrounding rock must have undergone plastic softening, so the area formed by the corresponding points must belong to the plastic softening zone. By analogy, the points corresponding to $E'O$ in the surrounding rock must only have elastic deformation, so the area formed by these points must belong to the elastic zone.

3.3.3. Deformation mechanism of surrounding rock in two zones

It is consistent with the deformation mechanism of the three zones of the actual surrounding rock mentioned above, when the corresponding point A'' of point A on the inner edge of the tunnel in the coordinate plane shown in Fig. 6 is located in the plastic softening stage on the corresponding loading path 1, the actual deformation zoning type of surrounding rock must be "two-zone". It should be noted that the three-stage model 1, 2, 3, 4 in Fig. 6 is the three-stage model 1, 2, 3, 4 in Fig. 5, and the purpose of separating them into separate maps is only to highlight the deformation mechanism of two zones of the actual surrounding rock.

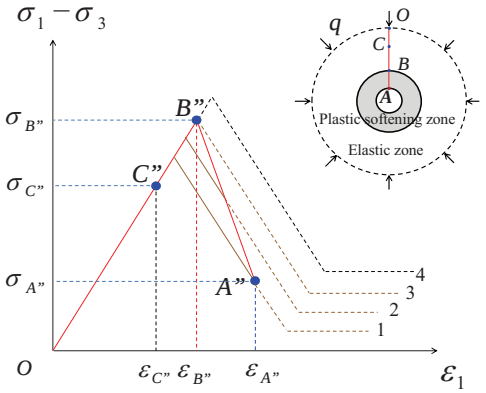

Fig. 6. Deformation mechanism of actual surrounding rock in two zones

At this time, because the final loading position of the rock at the inner edge of the tunnel is in the plastic softening stage of its loading path, there will be no broken zone in the tunnel surrounding rock, but only elastic zone and plastic softening zone.

3.3.4. Deformation mechanism of surrounding rock in one zone

Similarly, when the corresponding point A''' of point A on the inner edge of the tunnel in the coordinate plane shown in Fig. 7 is located in the linear elastic stage on the corresponding loading path 1, the actual deformation zoning type of surrounding rock must be "one-zone". The three-stage model 1, 2 in Fig. 7 is also separated from Fig. 5.

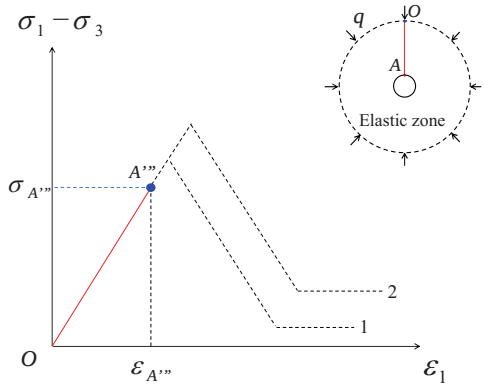

Fig. 7. Deformation mechanism of actual surrounding rock in one zones

To sum up, the actual deformation zoning type depends on the end position of the actual loading path of the rock at the inner edge of the tunnel on its corresponding test loading path. Therefore, the determination of the end position of the actual loading path of the rock at the inner edge of the tunnel is the key to determine the type of actual deformation zoning. Obviously, the above mechanism analysis can not give the end position of the actual loading path of the rock at the inner edge of the tunnel. The determination method of the actual deformation zoning type is given in combination with a specific example.

4. Determination method of actual deformation zone type of surrounding rock

According to the above analysis, the determination of the actual deformation zoning type depends on the position of the actual loading path end point of the rock in the inner edge of the tunnel, and the determination of this position involves a series of interrelated theories and tests. Specifically include the test of obtaining the peak strength and residual strength of the surrounding rock, drawing the peak strength fitting line and the residual strength fitting line in the $\sigma_1 - \sigma_3$ coordinate plane according to the peak strength and

residual strength under different confining pressure, and drawing the corresponding straight line in the above coordinate plane according to the straight line relationship between the circumferential stress and the radial stress in the elastic zone and the plastic softening zone. Finally, combined with the support strength, the end position of the actual loading path of the rock at the inner edge of the tunnel can be given, and the zoning type of the actual deformation zone of the surrounding rock will be obtained.

According to the above ideas, the following will be combined with specific examples to determine the actual deformation zoning type of tunnel surrounding rock.

4.1. Triaxial compression test of surrounding rock

The rock used to make the specimen is selected from the roof of 11-2 Coal Seam of Pan Yidong Mine in Huaibei mining area. The lithology is argillaceous, and the specimen size is 50–100 mm. Because of the low strength and low confining pressure of rock, it is difficult to obtain the post-peak part of the complete stress-strain curve. The excavation equivalent radius R_0 is 2.95 m, the elastic modulus E is 4.01 GPa, Poisson's ratio $\nu = 0.25$ and support load $p_s = 0.75$ MPa. According to the in-situ stress test results, the initial in-situ stress $q = 21.86$ MPa, the maximum principal stress of surrounding rock is 20.42 MPa, the minimum principal stress is 9.49 MPa and the intermediate principal stress is 17.55 MPa. The initial cohesion C_0 of surrounding rock is 11.57 MPa, and the residual cohesion C_b is 0.724 MPa.

The test is divided into 6 groups, each group has 3 tests, and the corresponding confining pressures are 0 MPa, 3 MPa, 7 MPa, 11 MPa, 15 MPa and 19 MPa respectively. From the three complete stress-strain curves obtained from each group of tests, an ideal curve can be selected as the complete stress-strain curve under the confining pressure. The σ_1 in the figure is the circumferential stress σ_θ of surrounding rock and σ_3 is the radial stress σ_ρ of surrounding rock. The compression test is carried out by using TAW-3000 microcomputer-controlled power servo rock triaxial testing machine, as shown in Fig. 8, and the complete stress-strain curve obtained from the six groups of tests is shown in Fig. 9. The corresponding peak strength and residual strength are shown in Table 1.

Fig. 8. TAW-3000 microcomputer servo-controlled triaxial rock testing machine

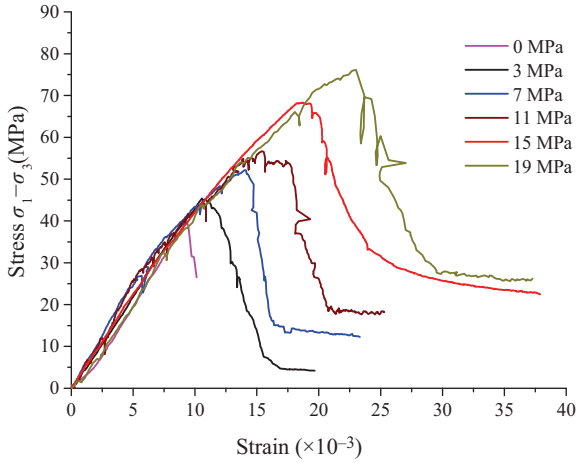

Fig. 9. Six stress-strain curves under confining pressures

Table 1. Mechanical strength parameter list of confining pressure

$\sigma_2 = \sigma_3$ (MPa)	σ_c (MPa) (Peak intensity)	σ_w (MPa) (Residual strength)
0	39.84603	/
3	48.36703	8.1
7	59.21081	22.5
11	67.67364	30.5
15	83.32177	46.5
19	95.15264	48.5

4.2. Fitting line between peak strength and residual strength

The coordinate plane $\sigma_1 - \sigma_3$ of surrounding rock is established, and the corresponding coordinate points are determined according to the peak intensity values of six kinds of confining pressure in Table 1. The peak intensity fitting line 1 and its mathematical expression (4.1) can be obtained as follows.

$$y = 2.942x + 38.383 \tag{4.1}$$

The corresponding coordinate points are determined from the residual strength values under five kinds of confining pressure in Table 1, and the residual strength fitting line 2 and its fomula (4.2) are obtained.

$$y = 2.620x + 2.400 \tag{4.2}$$

Fig. 10 is drawn based on the peak strength and residual strength of rock specimen obtained from triaxial compression test and their corresponding confining pressures. Ac-

cording to the above basic assumption (3), for the tunnel surrounding rock with completely consistent rock properties, the radial stress σ_ρ of the tunnel in Fig. 10 corresponds to the confining pressure σ_3, and the circumferential stress σ_θ of the tunnel can corresponds to the axial pressure σ_1. The peak strength fitting line 1 in Fig. 10 is the relationship line between the peak strength and the confining pressure (radial stress) of tunnel surrounding rock, and the residual strength fitting line 2 is the relationship line between the residual strength and the confining pressure of tunnel surrounding rock. For the peak strength fitting line 1, when there is a plastic softening zone in the surrounding rock, there must be only one point on the fitting line 1 corresponding to the boundary stress at the interface between the plastic softening zone and the elastic zone, and the abscissa and ordinate values of the point are equal to the values of the radial stress and the circumferential stress at the interface respectively. Similarly, there must be only one point on the residual strength fitting line 2 that corresponds to the boundary stress at the interface of plastic softening zone and broken zone, and the abscissa and ordinate values of this point are equal to the values of radial stress and circumferential stress at the interface respectively. Therefore, the actual deformation zoning type of tunnel surrounding rock can be analyzed according to the two fitting lines in Fig. 10 combined with the law of stress distribution in each deformation zone of surrounding rock.

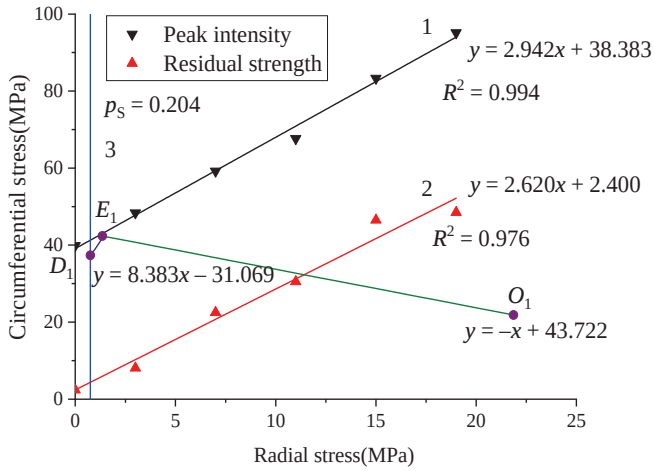

Fig. 10. Determination method of actual zoning type and boundary stress of tunnel surrounding rock

4.3. Determination of actual deformation zoning type and boundary stress

In order to obtain the coordinate points of the peak strength fitting line corresponding to the boundary stress at the interface between the plastic softening zone and the elastic zone in Fig. 10, and the corresponding coordinate points of the residual strength fitting

line corresponding to the boundary stress at the interface between the broken zone and the plastic softening zone, it is necessary to draw the deformation regions (elastic zone, plastic zone) corresponding to the in-situ stress and the properties of surrounding rock in the coordinate plane shown in Fig. 10. According to the intersection position of these lines (or curves) and the above two fitting lines, the actual deformation zoning type of surrounding rock can be accurately determined. The following is a detailed quantitative analysis.

4.3.1. Determination of stress at inner boundary of elastic zone

According to the axisymmetric elastic theory, there is a linear relationship between the radial stress and the circumferential stress in the elastic zone of the surrounding rock.

$$\sigma_{\theta e} = -\sigma_{\rho e} + 2q \tag{4.3}$$

In formula (4.3), the radial stress and circumferential stress in the elastic zone are respectively $\sigma_{\rho e}$ and $\sigma_{\theta e}$ in the elastic zone, q is the value of in-situ stress.

In the coordinate plane of Fig. 10, the coordinate point corresponding to O point on the outer boundary of the elastic zone in Fig. 2 is O_1 point. Based on this point, the relationship line O_1E_1 between radial stress and circumferential stress of the elastic zone along the radial direction of tunnel surrounding rock corresponding to formula (4.3) can be drawn. Because the interface between the elastic zone and the plastic softening zone belongs to both the elastic zone and the plastic softening zone, the corresponding coordinate point of the radial stress and the circumferential stress at the interface in the coordinate plane of Fig. 10 must be on line 1 and line O_1E_1 at the same time, so the abscissa and ordinate values of the intersection point between the two lines are the radial and circumferential stress values at the interface.

However, if the intersection E_1 is on the right side of the support strength line 3, it will be indicated that the plastic softening zone must exist. If the intersection E_1 is on the left side of the support strength line 3, it means that only elastic zone exists in the surrounding rock, because the support strength line 3 is the radial pressure from the support structure, corresponding to the inner edge of the tunnel, which is the minimum radial pressure in the surrounding rock. If the intersection E_1 happens to be on the intersection of line 1 and line 3, it indicates that the surrounding rock at the inner edge of the tunnel happens to have strength failure. By solving the equation (4.3) and the equation of line 1, the coordinates of point E_1 can also be obtained, which are (1.354, 42.366), MPa.

4.3.2. Determination of stress at the inner boundary of plastic hardening zone

The research in reference [41] shows that the relationship between the radial stress and the circumferential stress in the plastic softening zone along the radial direction of the tunnel is as follows:

$$\sigma_{\theta s} = (2K_s + \eta_1)\sigma_{\rho s} + D_0 \tag{4.4}$$

$$\begin{cases} D_0 = J_0 + T_0 \\ J_0 = 2(K_s)^{1/2} C_{E'} - 2(K_S)^{1/2} \varepsilon_{E'} M_C \dfrac{1+\eta_0}{1+\eta_1} \\ T_0 = -2\,(K_S+\eta_1)\,(K_S)^{1/2} \left[\dfrac{C_{E'}}{1-K_S} + \dfrac{\varepsilon_{E'} M_C (\eta_0+1)}{(\eta_1+1)(1-K_S)} \right] \end{cases} \tag{4.5}$$

In the formula (4.6), $\sigma_{\rho s}$ and $\sigma_{\theta s}$ are radial stress and circumferential stress in plastic softening zone respectively, φ_S is internal friction angle of rock in plastic softening zone and broken zone, η_0 and η_1 are expansion parameters of rock mass in elastic zone and plastic softening zone respectively, K_s is the slope of the fitting line for the compressive strength of the plastic softening zone, M_C represents the softening modulus of cohesion of the plastic softening zone. $\varepsilon_{E'}$ is circumferential strain value corresponding to point E' in Fig. 5, $C_{E'}$ is the cohesion corresponding to point E' in Fig. 5, which is initial cohesion C_0. According to correlation flow rule, $\varphi_S = \psi_S$ can be obtained, so there is the following relationship:

$$\eta_1 = \frac{1+\sin\psi_S}{1-\sin\psi_S} = \frac{1+\sin\varphi_S}{1-\sin\varphi_S} = K_S \tag{4.6}$$

M_C can be calculated according to the formula (4.7) according to the reference [42].

$$M_C = \frac{\left[\sigma_{\rho b} - 2(K_S)^{1/2} \dfrac{C_{E'}}{1-K_S}\right](1-K_S)(K_S+\eta_1)}{2\,(K_S)^{1/2}\,\varepsilon_{E'}(1+\eta_0)} \tag{4.7}$$

$\sigma_{\rho b}$ is the radial stress at the interface between plastic softening zone and elastic zone,D_0 is the intercept of the relationship between radial stress and circumferential stress of surrounding rock on the longitudinal coordinate axis in Fig. 10. According to formula (4.6), it is known that K_s and η_1 are only related to the internal friction angle φ_S. The reference [42] shows that according to the analysis of the experimental data about the internal friction angle of rock in the post-peak stage in 18 published literatures in recent years, it is concluded that the internal friction angle in the plastic softening stage is approximately constant, so the K_s and η_1 in formula (4.5) are approximately constant. $C_{E'}$ and $\varepsilon_{E'}$ in formula (4.7) are the cohesion and circumferential linear strain of surrounding rock at the interface between plastic softening zone and elastic zone (the peak point of complete stress-strain curve), so these two parameters are also fixed values for the surrounding rock of specific tunnel. $\sigma_{\rho b}$ in formula (4.7) is the boundary radial stress at the interface between plastic softening zone and elastic zone. According to reference [41], this stress value is only related to the in-situ stress and the properties of surrounding rock, so for a specific tunnel, $\sigma_{\rho b}$ is also a constant.

According to the above analysis, for a specific tunnel, J_0 and T_0 in formula (4.5) are constant, so D_0 in formula (4.4) is also constant, and K_s and η_1 are also constant at this time, so it can be concluded that there is a linear relationship between $\sigma_{\theta s}$ and $\sigma_{\rho s}$, which is an oblique line in the coordinate plane shown in Fig. 10. Therefore, the position of the relationship line between the circumferential stress and the radial stress of plastic softening

zone in the $\sigma_1 - \sigma_3$ coordinate plane is only determined by the in-situ stress and the properties of surrounding rock.

Because the corresponding coordinate point of radial stress and circumferential stress of rock in the coordinate plane of Fig. 10 should be on the straight line of line 1, line O_1E_1 and the relationship line between $\sigma_{\theta s}$ and $\sigma_{\rho s}$ in the plastic softening zone, the point E_1 is the intersection of three straight lines. Because point E_1 corresponds to the peak value of circumferential stress in surrounding rock (point E_1 is corresponding to points E and E' in Fig. 5), the point E_1 in Fig. 10 must be the upper end of the straight line between $\sigma_{\theta s}$ and $\sigma_{\rho s}$ in the plastic softening zone.

Thus, according to formula (4.3), it can be inferred that the position of radial stress and circumferential stress relationship line O_1E_1 in elastic zone depends on the value of in-situ stress q, the position of peak strength fitting line 1 depends on the properties of surrounding rock, and the position of circumferential stress and radial stress relationship line E_1D_1 in plastic softening zone is determined by both in-situ stress and surrounding rock properties. Therefore, the values of radial stress and circumferential stress corresponding to the rock particles at the interface between the elastic zone and the plastic softening zone (the coordinate values of $\sigma_{\theta s}$ and $\sigma_{\rho s}$ corresponding to the point E_1 in Fig. 10 are only determined by the specific in-situ stress field and the properties of tunnel surrounding rock.

After the location of E_1 point is determined, it is also necessary to determine the slope $(2K_s + \eta_1)$ of the straight line E_1D_1, which is related to the internal friction angle φ_S of rock in the stage of plastic softening, so the value of φ_S needs to be determined.

Meanwhile, literature [42] analyzed 18 achievements in studying the post-peak characteristics of rocks and concluded that the internal friction angle remains approximately unchanged after rock fracture. Therefore, the internal friction angle in the plastic softening stage is approximately equal, it can be calculated by the average value. From formulas (4.1) and (4.2), it can be seen that the slopes of fitting lines 1 and 2 are not completely the same, indicating that there is a slight difference in the internal friction angle between the peak point and the residual point. Therefore, the average slope of the two lines can be used to calculate the internal friction angle, as follows:

$$K_S = (2.942 + 2.620)/2 = 2.781 \tag{4.8}$$

According to the Mohr–Coulomb criterion, the relationship between the slope and the internal friction angle is as follows:

$$K_S = \frac{1 + \sin\varphi}{1 - \sin\varphi} \tag{4.9}$$

By substituting $K_S = 2.781$ into the above formula and solving, the value of internal friction angle φ_S of surrounding rock in plastic softening stage can be obtained.

$$\varphi_S = 28.117 \tag{4.10}$$

Therefore, the slope of the relation line E_1D_1 between $\sigma_{\theta s}$ and $\sigma_{\rho s}$ is as follows:

$$(2K_S + h_1) = 8.343 \tag{4.11}$$

Substituting the slope value of line E_1D_1 and point E_1 coordinates into formula (4.4), the specific formula of line E_1D_1 can be calculated.

$$\sigma_{\theta s} = 8.343\sigma_{\rho s} + 31.070 \tag{4.12}$$

According to the above equations, the relationship line E_1D_1 between circumferential stress and radial stress in the plastic softening zone can be drawn, and the point D_1 is the intersection of line E_1D_1 and support strength line 3. By substituting the support load $p_s = 0.75$ MPa into equation (4.12), the ordinate of point D_1 (the circumferential stress of the inner edge of the tunnel) can be obtained to be 37.327 MPa. Therefore, the coordinate value of point D_1 is (0.75, 37.327), MPa.

As can be seen from Fig. 10, because D_1 is located in the area between lines 1 and 2, and there is no intersection between E_1D_1 and line 2, it shows that there is no broken zone in the surrounding rock, and only plastic softening deformation occurs in a certain area on the inside of the tunnel. Therefore, the actual deformation zoning type of this tunnel is two zones.

4.4. Verification and analysis of calculation results

In order to verify the scientific soundness of this method, the field measured data of this example are substituted into references [18] and [22] for calculation respectively, and the stress values at the elasto-plastic junction of surrounding rock obtained are shown in Table 2.

Table 2. Comparison of partition radii under different mechanical models

Method	$(\sigma_\rho)_{E_1}$	$(\sigma_\theta)_{E_1}$	$(\sigma_\rho)_{D_1}$	$(\sigma_\theta)_{D_1}$
Method of this paper	1.354	42.366	0.750	37.327
Reference [18] D-P criterion	1.133	42.589	0.750	39.249
Reference [22] M-C criterion	1.423	42.298	0.750	40.443

The analytical formula of stress in each zone of surrounding rock in reference [18] is based on the three-zone theory based on Drucker–Prager criterion. The elastic-plastic analytical solution of surrounding rock in reference [22] is based on the three-zone theory based on Mohr–Coulomb criterion. The data in Table 2 show that the values of radial stress and circumferential stress at E_1 point at the junction of elastic zone and plastic zone of surrounding rock obtained by the two methods in the literature are highly consistent with those obtained by this method, and the error between D_1 radial stress and circumferential stress at the inner wall of tunnel is small, so the reliability of this method has been proved.

If there is a broken zone in the tunnel surrounding rock, there must be an intersection between the residual strength fitting line 2 and the relationship line E_1D_1 of circumferential stress and radial stress in the plastic softening zone in the $\sigma_1 - \sigma_3$ coordinate plane shown in Fig. 10. Since the position of line 2 in the coordinate plane is only determined by the

properties of surrounding rock, combined with the above analysis, the values of radial stress and circumferential stress at the interface between plastic softening zone and broken zone also depend on the specific in-situ stress field and the properties of tunnel surrounding rock.

To sum up, when the actual in-situ stress and surrounding rock properties at a certain tunnel are known, the relationship lines between radial stress and circumferential stress in each deformation zone of the tunnel surrounding rock, as well as the fitting lines for peak stress and residual strength of the surrounding rock, will be determined, and the intersection coordinates of all curves will also be fixed. Therefore, the stress values at the boundaries of each deformation zone of the tunnel surrounding rock are determined by rock mechanical properties and in-situ stress, and the changes in support parameters only change the type and stress values of the surrounding rock at the tunnel wall.

5. Discussion

The above analysis process clearly demonstrates that the actual deformation zoning type of surrounding rock is only related to in-situ stress and the properties of surrounding rock, and does not involve other factors, which is of great significance to the quantitative design of tunnel surrounding rock support parameters. This conclusion is further supported by the way of obtaining different deformation zoning types of surrounding rock by changing the properties of surrounding rock and the value of in-situ stress.

5.1. Influence of rock mechanical properties on deformation zoning type of surrounding rock

At this time, it can be divided into two situations: the decrease of surrounding rock strength and the increase of surrounding rock strength. The following is an example of the decrease of surrounding rock strength.

In Fig. 10, when the compressive strength and residual strength of surrounding rock are reduced, the fitting lines of the relationship between radial stress and circumferential stress after strength reduction are line 4 and line 5 in Fig. 11 respectively. Because the in-situ stress does not change, it can be seen from formula (4.3) that the relationship between radial stress and circumferential stress in the radial path of elastic zone is still the straight line O_1E_1 in Fig. 10. Because the fitting line 4 overall downward translation, the position of the E_2 point moves to the right, and the direct result of E_2 point moving to the right is that the relationship between radial stress and circumferential stress in the radial path of the plastic softening zone intersects with the residual strength fitting line 5 at point C_2 in Fig. 12. Because the fitting line 5 is the residual strength fitting line under different confining pressure, there must be a broken zone as long as the C_2E_2 line intersects the fitting line 5. The C_2 point in Fig. 11 corresponds to the position of the interface between the plastic softening zone and the broken zone, and its horizontal and longitudinal coordinates are the radial stress and circumferential stress at the interface. A_2C_2 is the relationship between radial stress and circumferential stress in the radial path of the broken zone. The line A_2C_2

intersects with support strength line 3 at point A_2, and the radial stress corresponding to A_2 is the support pressure.

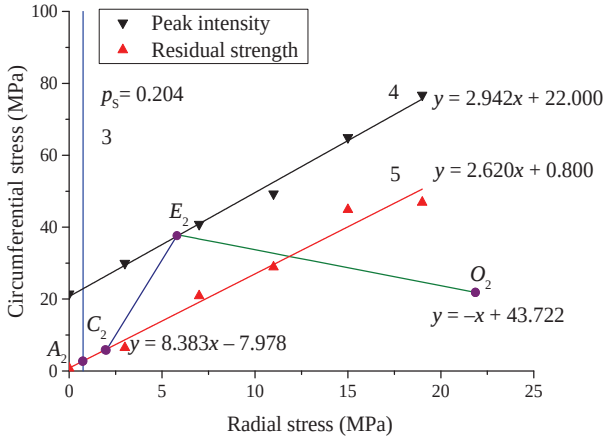

Fig. 11. The influence of compressive strength and residual strength reduction on deformation zone

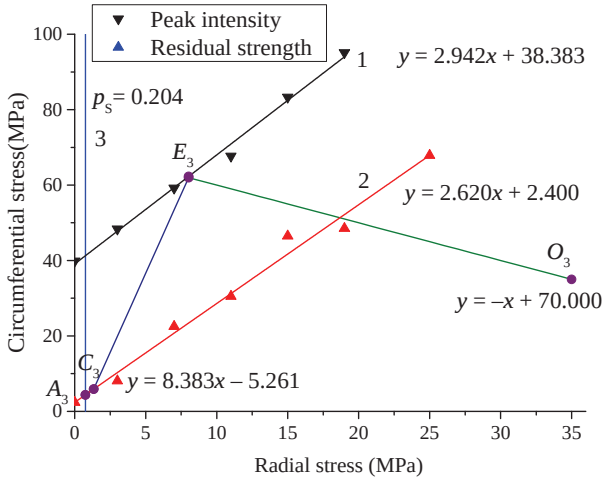

Fig. 12. The effect of increased in-situ stress on the actual deformation zone

The results show that due to the decrease of surrounding rock strength, the surrounding rock has evolved from two deformation zones to three deformation zones, and the number of zones has increased. In conclusion, when the strength of surrounding rock decreases, the number of zones of surrounding rock may increase; similarly, when the strength of surrounding rock increases, the number of zones of surrounding rock may decrease.

5.2. Influence of in-situ stress on deformation zoning type of surrounding rock

Take the case of increasing the value of in-situ stress as an example. Compared with Fig. 10, the in-situ stress corresponding to Fig. 12 is increased to hydrostatic pressure 35 MPa, which results in the overall right shift of the O_1E_1 line and C_1E_1 line in Fig. 10 to the position of O_3E_3 line and C_3E_3 line in Fig. 12. This leads to the intersection point C_3 between the relationship line C_3E_3 of circumferential stress and radial stress in the plastic softening zone and the fitting line 2 of residual strength, forming the actual deformation zone 3.

The results show that due to the increase of in-situ stress, the surrounding rock changes from two deformation zones to three deformation zones, and the number of zones increases. Therefore, increasing the value of in-situ stress may increase the number of deformation zones of surrounding rock; similarly, decreasing the value of in-situ stress may decrease the number of deformation zones of surrounding rock.

To sum up, the stress values at the boundaries of each deformation zone of the tunnel surrounding rock are only related to the mechanical properties and in-situ stress of the surrounding rock, and can be quantitatively analyzed.

6. Conclusions

Based on the requirements of safe and efficient production of coal mine and disaster prevention, the actual deformation evolution law of tunnel surrounding rock is systematically analyzed. Based on the current general three zoning theory, the experimental determination method of actual deformation zoning type and boundary stress of tunnel surrounding rock are obtained, and the influencing factors of actual zoning type are studied. The specific conclusions are as follows:

1. Through expounding the characteristics and differences of rock test loading path and actual loading path of surrounding rock in the process of tunnel forming, the differences between basic deformation zoning type and actual deformation zoning type of surrounding rock are analyzed, and the forming mechanism of actual deformation zoning type of surrounding rock of tunnel is revealed.
2. Based on the axisymmetric elasto-plastic theory and triaxial compression tests under different confining pressures, this paper puts forward the actual deformation zoning types of surrounding rock and the determination method of the boundary stress of surrounding rock deformation zones. The results can provide a theoretical basis for further determining the zoning boundary radius of surrounding rock.
3. The paper reveals the change rule of the actual deformation zone type of surrounding rock with the in-situ stress and the basic mechanical properties of the surrounding rock, and gives the theoretical analysis method to determine the actual deformation zone number of the surrounding rock. The results can provide reference for decision-making of supporting scheme and quantitative design of supporting parameters.

Acknowledgements

This study was supported by the Major Project Of Natural Science Research In Colleges And Universities Of Anhui Provincial Department of Education (KJ2021ZD0053), the National Natural Science Foundation of China (51904012), the Open Fund of State Key Laboratory of Mining Response and Disaster Prevention and Control in Deep Coal Mine (SKLMRDPC19KF02), the Project Supported By Scientific Research Activities Of Postdoctoral Researchers In Anhui Province (2022B640), the Research Project on Ningzheng Coal Mine Large Buried Deep Ultra-Thick Coal Seam Driving tunnel Along Goaf Floor Key Support Technology Of Huaneng Qingyang Coal Power Co., Ltd.(HNQMHTY-051-2022-JZ01), the Research Project On "Three Soft" Coal Seam Mining tunnel Support Technology Research Project Of Daliu Coal Mine Co., Ltd. (HNMYKJ19-04), and The Project Of Research On Large Deformation Mechanism And Control Technology Of Goaf Side Entry In Xichuan Coal Mine With Complex Geological Conditions Of Huaneng Group Headquarters (HNKJ21-HF05).

References

[1] B. Indraratna and P. K. Kaiser, "Design for grouted rock bolts based on the convergence control method", *International Journal of Rock Mechanics and Mining Sciences & Geomechanics Abstracts*, vol. 27, no. 4, pp. 269–281, 1990, doi: 10.1016/0148-9062(90)90529-B.

[2] C.C. Torres, "Analytical and numerical study of the mechanics of rockbolt reinforcement around tunnels in rock masses", *Rock Mechanics and Rock Engineering*, vol. 42, pp. 175–228, 2009, doi: 10.1007/s00603-009-0178-2.

[3] J.J. Park, I.S. Cho, I.M. Lee, and S.W. Lee, "Tunnel reinforcement by using pressure-induced inflatable pipes method", *Journal of Geotechnical and Geoenvironmental Engineering,* vol. 138, no. 12, pp. 1483–1491, 2012, doi: 10.1061/(ASCE)GT.1943-5606.0000725.

[4] H. Kang, Y. Wu, F. Gao, P. Jiang, P. Cheng, X. Meng, and Z. Li, "Mechanical performances and stress states of rock bolts under varying loading conditions", *Tunnelling and Underground Space Technology*, vol. 52, pp. 138–146, 2016, doi: 10.1016/j.tust.2015.12.005.

[5] J.S. Zhang, Y. Lu, H.L. Zhang, Y.D. Yang, and Y.S. Bu, "Experimental study on fatigue mechanical properties of sandstone after dry and wet cycle", *Archives of Civil Engineering*, vol. 68, no. 4, pp. 377–387, 2022, doi: 10.24425/ace.2022.143044.

[6] Y.R. Zheng and F.Y. Dong, Eds., *Design Guide of shotcrete support for underground engineering*. Beijing: China Railway Press, 1988.

[7] E. Hoek and E. T. Brown, "Practical estimates of rock mass strength", *International Journal of Rock Mechanics and Mining Sciences,* vol. 34, no. 8, pp. 1165–1186, 1997, doi: 10.1016/S1365-1609(97)80069-X.

[8] R.R. Osgoui and P. Oreste, "Elasto-plastic analytical model for the design of grouted bolts in a Hoek–Brown medium", *International Journal For Numerical and Analytical Methods in Geomechanics*, vol. 34, no. 16, pp. 1651–1686, 2010, doi: 10.1002/nag.823.

[9] A. Serrano, C. Olalla, and I. Reig, "Convergence of circular tunnels in elastoplastic rock masses with non-linear failure criteria and non-associated flow laws", *International Journal of Rock Mechanics and Mining Sciences*, vol. 48, no. 6, pp. 878–887, 2011, doi: 10.1016/j.ijrmms.2011.06.008.

[10] S. Kwon, C.S. Lee, S.J. Cho, S.W. Jeon, and W.J. Cho, "An investigation of the excavation damaged zone at the KAERI underground research tunnel", *Tunnelling and underground Space Technology,* vol. 24, no. 1, pp. 1–13, 2009, doi: 10.1016/j.tust.2008.01.004.

[11] M.J. Leitman and P. Villaggio, "Plastic zone around circular holes", *Journal of Engineering Mechanics*, vol. 135, no. 12, pp. 1467–1471, 2009, doi: 10.1061/(ASCE)EM.1943-7889.0000062.

[12] L. Zhao, Z. Cui, R. Peng, T. Wei, L. Wang, and D. Liu, "Deformation characteristics and grouting control technology of reused tunnel in a fully mechanized coalface with large mining height", *Applied Sciences*, vol. 13, no. 3, art. no. 1951, 2023, doi: 10.3390/app13031951.

[13] N.J. Ma and Y.D. Zhang, "A new analysis on ground pressures around openings", *Chinese Journal of Rock Mechanics and Engineering*, vol. 15, no. 1, no. 84-89, 1996.

[14] A. Fahimifar and H. Soroush, "A theoretical approach for analysis of the interaction between grouted rockbolts and rock masses", *Tunnelling and Underground Space Technology*, vol. 20, no. 4, pp. 333–343, 2005, doi: 10.1016/j.tust.2004.12.005.

[15] G.S. Yao, J.P. Li, and S.C. Gu, "Analytic solution to deformation of soft rock tunnel considering dilatancy and plastic softening of rock mass", *Rock and Soil Mechanics*, vol. 30, no. 2, pp. 463–467, 2009.

[16] G. Walton, M. Lato, M. Anschütz, M.A. Perras, and M.S. Diederichs, "Non-invasive detection of fractures, fracture zones, and rock damage in a hard rock excavation—Experience from the Äspö Hard Rock Laboratory in Sweden", *Engineering Geology*, vol. 196, pp. 210–221, 2015, doi: 10.1016/j.enggeo.2015.07.010.

[17] S.K. Paul, "Numerical models of plastic zones and associated deformations for elliptical inclusions in remote elastic loading–unloading with different R-ratios", *Engineering Fracture Mechanics*, vol. 152, pp. 72–80, 2016, doi: 10.1016/j.engfracmech.2015.12.008.

[18] L. Chen, X.B. Mao, M. Li, and Y.L. Chen, "Elastoplastic analysis of cracked surrounding rock in deep tunnel based on Drucker–Prager criterion", *Journal of China Coal Society*, vol. 42, no. 2, pp. 484–491, 2017, doi: 10.13225/j.cnki.Jccs.2016.6029.

[19] Q. Zhang, B. Jiang, and H. Lv, "Analytical solution for a circular opening in a rock mass obeying a three-stage stress–strain curve", *International Journal of Rock Mechanics and Mining Sciences*, vol. 86, pp. 16–22, 2016, doi: 10.1016/j.ijrmms.2016.03.013.

[20] B. Sun, P. Zhang, R. Wu, M. Fu, and Y. Ou, "Research on the overburden deformation and migration law in deep and extra-thick coal seam mining", *Journal of Applied Geophysics*, vol. 190, art. no. 104337, 2021, doi: 10.1016/j.jappgeo.2021.104337.

[21] J. F. Zou and Z. Q. Xia, "Closed-form solution for cavity expansion in strain-softening and undrained soil mass based on the unified strength failure criterion", *International Journal of Geomechanics*, vol. 17, no. 9, 2017, doi: 10.1061/(ASCE)GM.1943-5622.0000927.

[22] G.S. Yao, J.P. Li, and S.C. Gu, "Analytic solution to deformation of soft rock tunnel considering dilatancy and plastic softening of rock mass", *Rock and Soil Mechanics*, vol. 30, no. 2, pp. 463–467, 2009.

[23] J.L. Pan, Z.N. Gao, and F.H. Ren, "Effect of strength criteria on surrounding rock of circular tunnel considering strain softening and dilatancy", *Journal of China Coal Society*, vol. 43, no. 12, pp. 3293–3301, 2018.

[24] L.R. Alejano, A. Rodríguez-Dono, and M. Veiga, "Plastic radii and longitudinal deformation profiles of tunnels excavated in strain-softening rock masses", *Tunnelling and Underground Space Technology*, vol. 30, pp. 169–182, 2012, doi: 10.1016/j.tust.2012.02.017.

[25] Y. Li, S. Cao, N. Fantuzzi, and Y. Liu, "Elasto-plastic analysis of a circular borehole in elastic-strain softening coal seams", *International Journal of Rock Mechanics and Mining Sciences*, vol. 80, pp. 316–324, 2015, doi: 10.1016/j.ijrmms.2015.10.002.

[26] M. Ranjbarnia, A. Fahimifar, and P. Oreste, "Practical method for the design of pretensioned fully grouted rockbolts in tunnels", *International Journal of geomechanics*, vol. 16, no. 1, art. no. 04015012, 2016, doi: 10.1061/ (ASCE)GM.1943-5622.0000464.

[27] R. Fei, L. Peng, C. Zhang, J. Zhang, and P. Zhang, "Centrifuge model test of parallel shield underneath high-speed railway tunnel", *Archives of Civil Engineering*, vol. 68, no. 3, pp. 661–677, 2022, doi: 10.24425/ace.2022.141909.

[28] S. Hao, R. Fei, and J. Yu, "Mechanical characteristics of ultra-shallow buried high-speed railway tunnel in broken surrounding rock during construction", *Archives of Civil Engineering*, vol. 68, no. 3, pp. 645–659, 2022, doi: 10.24425/ace.2022.141908.

[29] S.L. Chen, Y.N. Abousleiman, and K.K. Muraleetharan, "Closed-form elastoplastic solution for the wellbore problem in strain hardening/softening rock formations", *International Journal of Geomechanics*, vol. 12, no. 4, pp. 494–507, 2012, doi: 10.1061/(ASCE)GM.1943-5622.0000157.

[30] Z.N. Gao, X.R. Meng, and Z.L. Fu, "Elasto-plastic analysis on surrounding rock of tunnels based on seepage, strain softening and dilatancy", *Journal of Chongqing University*, vol. 37, no. 1, pp. 96–101, 2014.

[31] D. Palumbo, R. De Finis, F. Ancona, and U. Galietti, "Damage monitoring in fracture mechanics by evaluation of the heat dissipated in the cyclic plastic zone ahead of the crack tip with thermal measurements", *Engineering Fracture Mechanics*, vol. 181, pp. 65–76, 2017, doi: 10.1016/j.engfracmech.2017.06.017.

[32] M.B. Reed, "The influence of out-of-plane stress on a plane strain problem in rock mechanics", *International Journal for Numerical and Analytical Methods in Geomechanics*, vol. 12, no. 2, pp. 173–181, 1988, doi: 10.1002/nag.1610120205.

[33] K.H. Park, "Similarity solution for a spherical or circular opening in elastic-strain softening rock mass", *International Journal of Rock Mechanics and Mining Sciences,* vol. 71, pp. 151–159, 2014, doi: 10.1016/j.ijrmms.2014.07.003.

[34] L. Cui, J.J. Zheng, R.J. Zhang, and Y.K. Dong, "Elasto-plastic analysis of a circular opening in rock mass with confining stress-dependent strain-softening behaviour", *Tunnelling and Underground Space Technology,* vol. 50, pp. 94–108, 2015, doi: 10.1016/j.tust.2015.07.001.

[35] M.R. Zareifard, "Ground reaction curve for deep circular tunnels in strain-softening mohr–coulomb rock masses considering the damaged zone", *International Journal of Geomechanics,* vol. 20, no. 10, art. no. 04020190, 2020, doi: 10.1061/(ASCE)GM.1943-5622.0001822.

[36] F. Huang, H.H. Zhu, Q.W. Xu, Y.C. Cai, and X.Y. Zhuang, "The effect of weak interlayer on the failure pattern of rock mass around tunnel-Scaled model tests and numerical analysis", *Tunnelling and Underground Space Technology*, vol. 35, pp. 207–218, 2013, doi: 10.1016/j.tust.2012.06.014.

[37] A. Singh, C. Kumar, L.G. Kannan, K.S. Rao, and R. Ayothiraman, "Estimation of creep parameters of rock salt from uniaxial compression tests", *International Journal of Rock Mechanics and Mining Sciences*, vol. 107, pp. 243–248, 2018, doi: 10.1016/j.ijrmms.2018.04.037.

[38] M.F. Cai, M.C. He, and D.Y. Liu, Eds., *Rock mechanics and engineering.* Beijing: Science Press, 2013.

[39] M.A. Perras and M.S. Diederichs, "Predicting excavation damage zone depths in brittle rocks", *Journal of Rock Mechanics and Geotechnical Engineering*, vol. 8, no. 1, pp. 60–74, 2016, doi: 10.1016/j.jrmge.2015.11.004.

[40] W.Q. Ma and T.X. Wang, "Instability mechanism and control countermeasure of a cataclastic tunnel regenerated roof in the extraction of the remaining mineral resources: a case study", *Rock Mechanics and Rock Engineering*, vol. 52, no. 7, pp. 2437–2457, 2019, doi: 10.1007/s00603-018-1705-9.

[41] W. Jing, R. Guo, R.S. Yang, L.W. Jing, and W.P. Xue, "A theoretical analysis of surrounding rock deformation of deep soft rock tunnel based on rock rheology and strain softening", *Journal of Mining & Safety Engineering*, vol. 38, no. 3, pp. 538–546, 2021, doi: 10.13545/j.cnki.jmse.2020.0463.

[42] W. Jing, S. X. Liu, R.S. Yang, L.W. Jing, and W.P. Xue, "Mechanism of aging deformation zoning of surrounding rock in deep high stress soft rock tunnel based on rock creep characteristics", *Journal of Applied Geophysics*, vol. 202, art. no. 104632, 2022, doi: 10.1016/j.jappgeo.2022.104632.

Received: 2023-04-06, Revised: 2023-08-17